SURFACE INFLUENCE UPON VERTICAL PROFILES IN THE NOCTURNAL BOUNDARY LAYER

J.R. GARRATT

CSIRO Division of Atmospheric Physics, P.O. Box 77, Mordialloc, Australia, 3195

(Received in final form 2 March, 1983)

Abstract. Near-surface wind profiles in the nocturnal boundary layer, depth h, above relatively flat, tree-covered terrain are described in the context of the analysis of Garratt (1980) for the unstable atmospheric boundary layer. The observations at two sites imply a surface-based transition layer, of depth z_*, within which the observed non-dimensional profiles Φ_M^0 are a modified form of the inertial sub-layer relation $\Phi_M(z/L) = (1 + 5z/L)$ according to

$$\Phi_M^0 \simeq (1 + 5z/L) \exp [-0.7 (1 - z/z_*)],$$

where z is height above the zero-plane displacement and L is the Monin–Obukhov length.

At both sites the depth z_* is significantly smaller than the appropriate neutral value (z_{*N}) found from the previous analysis, as might be expected in the presence of a buoyant sink for turbulent kinetic energy.

1. Introduction

In a recent paper (Garratt, 1980 – G80), observations from two towers situated 5 km apart in relatively flat, tree-covered terrain – the Koorin experiment (Clarke and Brook, 1979) – were used to investigate flux-profile relations in the height range z/z_0 from 5 to 85, z being height above the zero-plane displacement and z_0 the aerodynamic roughness length. The analysis, which was confined to the daytime atmospheric boundary layer (ABL), confirmed that a lower height limit exists (at $z = z_*$) to the validity of the Monin–Obukhov functions $\Phi_{M,H}(z/L)$ in unstable conditions and, by implication, of the logarithmic wind law in neutral conditions. Here L is the Monin–Obukhov length, whilst subscripts M and H refer to momentum and heat transfer, respectively. The results were consistent with the level z_* marking a separation between the inertial sub-layer above and a transition layer below, both of which constitute the inner layer, or atmospheric surface layer.

For wind at both sites, the depth z_* was found to be approximately constant in unstable conditions and equal to 3δ, δ being the tree spacing. The values $z_*/z_0 \simeq 35$ and 150 at the denser (M2, with $z_0 = 0.9$ m) and less dense (M1, with $z_0 = 0.4$ m) surfaces respectively, compared with a value of about 10 for high-density vegetation (the Thetford forest) inferred from the results of Raupach (1979). Within the transition layer, the observed non-dimensional profiles Φ^0 were well represented by

$$\Phi^0 = \Phi(z/L) \exp \{-\alpha_1 (1 - z/z_*)\} \qquad z \leq z_* \tag{1}$$

both for wind and temperature with $\alpha_1 = 0.7$, where $\Phi(z/L)$ is the profile form in the inertial sub-layer. The functional form of Equation (1) was obtained from a non-rigorous dimensional argument. It implies a 'kink' in the $\Phi^0/\Phi(z/L)$ variation with z/z_* at $z = z_*$,

Boundary-Layer Meteorology **26** (1983) 69–80. 0006–8314/83/0261–0069$01.80.

which in practice would be smoothed by the turbulent mixing process. Equation (1) should be interpreted mainly as a convenient interpolation formula for velocity gradients immediately above rough surfaces, and is retained here for direct comparison of the present analysis with that of the daytime data.

The observations used by G80 were made in the unstable ABL, of depth h varying between 1500–2500 m, implying the depth of the atmospheric surface layer $h_s \simeq 150$–250 m. Thus all of the observations (maximum level $z \simeq 43$ m) were made well within the surface layer, where $\Phi(z/L)$ has been well determined from experiments above low-z_0 surfaces. In contrast, little was known of the evolutionary nature and the depth h of the nocturnal boundary layer (NBL) at the Koorin experiment, so that nighttime observations were excluded from the analysis of G80. Details of the Koorin NBL are now available (e.g., Garratt, 1982), and the present paper describes the extension of the near-surface profile analysis to the nocturnal situation, but restricted to the momentum case.

2. The Stable Surface Layer

Within the inertial sublayer, the profile form suggested by Monin and Obukhov (1954) is:

$$\Phi(z/L) = \Phi(0) + \beta z/L \tag{2}$$

for $z < h_s$, h_s being the height of the surface layer. For a neutral ABL, h_s is approximately 0.1 h (e.g., Tennekes and Lumley 1972; p. 162) and of similar magnitude in the NBL if we take the suggested relation of Zeman (1979), viz:

$$h_s/h = \frac{0.3}{1 + (h/L)^{-1}} \tag{3}$$

with $h/L \sim 1$ (Garratt, 1982). Note that Equation (3) implies $h_s/L \to 0.3$ as $h/L \to \infty$.

Observations above low-z_0 surfaces generally support Equation (2) for $z/L \lesssim 1$ (e.g., Webb, 1970; Businger *et al.*, 1971; Hicks, 1976) with

$$\Phi(0) = 1; \qquad 5 \lesssim \beta \lesssim 10$$

for wind and temperature. Garratt and Brost (1981) give a summary of β values, with the suggestion that these may be influenced by radiative cooling effects (their Table 7). Both Webb (1970) and Hicks (1976) discussed the breakdown of Equation (2) at larger values of z/L, but Equation (3) with $h/L = 3$ (typical of the mid-latitude NBL: see Garratt, 1982) implies $h_s/L \simeq 0.25$, so that their observations cannot be representative of the surface layer, but rather of the core of the (very shallow) NBL. Indeed the validity of Equation (2) out to $z/L \simeq 1$ implies that the profile form above the surface layer and into the central region of the NBL does not deviate significantly from the loglinear form. At extreme stability, the linear profile form deduced by Hicks (1976) is probably representative of the bulk of the NBL (e.g., Zeman, 1979) rather than the surface layer itself.

3. Koorin NBL

3.1 General features

The nocturnal turbulent boundary layer occurs frequently over land under clear skies when the geostrophic wind is not too low. Under these conditions it is possible to distinguish a shallow, fully-turbulent layer persisting from sunset to sunrise. Because of its time-evolving nature, the NBL may never reach steady-state (e.g., Zeman 1979; Nieuwstadt and Tennekes, 1981) and it may be affected significantly by drainage flows (e.g., Brost and Wyngaard, 1978). In addition, long-wave radiative cooling may be an important influence, particularly on flow dynamics above the NBL and on surface-layer properties (Garratt and Brost, 1981).

During the Koorin experiment, skies were generally clear at night with average geostrophic winds varying between 5 and 17 m s^{-1}. Of thirty nights' observations, only three have an NBL persisting for more than a few hours after sunset (approximately 1800 local time); several have intermittent periods with non-zero surface fluxes occurring around midnight. We follow Garratt (1982) and use in the present analysis only the three nights mentioned above. For two of these, turbulent activity ceased abruptly around midnight, apparently related to the passage of a sea-breeze front propagating inland from the coastline 200 km distant.

Evidence discussed by Garratt (1982) suggested a significant influence of drainage flow upon the scaled depth of the NBL, the actual depth h, taken as the height where the gradient Richardson number Ri = 0.25*, varying, typically, between 100–250 m. Equation (3) implies, with $h/L \simeq 1$ (Garratt, 1982), that $h_s \simeq 15$–40 m compared to the probable daytime range of 150–250 m.

3.2 Observations

Profile observations were made at two towers, M1 and M2, separated by 5 km, with night-time surface fluxes measured by eddy covariance techniques at M2 only. In order to utilise wind profile data at site M1, indirect estimates of friction velocity u_* and sensible heat flux H were made as described in the Appendix. All of the data used in the present paper can be found in Clarke and Brook (1979). Values of d, the zero-plane displacement, were taken as 4.8 and 7.1 m at M1 and M2 respectively (as used in G80). Temperature profile data (available at M1 only) in the non-dimensional form Φ_H^0 are not presented here since these were found to be excessively scattered. The major source of the scatter probably resides in the relatively small values of the turbulent temperature scale θ_* observed at night ($\simeq -0.1$ °C) compared to daytime ($\simeq 0.5$ °C), and the consequent larger relative errors in Φ_H^0.

Tower-averaged fluxes and estimates of h for the relevant three nights (Days 7/8; 27/28, and 28/29) can be found in Appendix 2 of Garratt (1982). Turbulent fluxes

* This value is taken as representative of the possible range $0.13 \lesssim \mathrm{Ri}_c \lesssim 0.5$, where Ri_c is the critical value, although h is not very sensitive to values within the range.

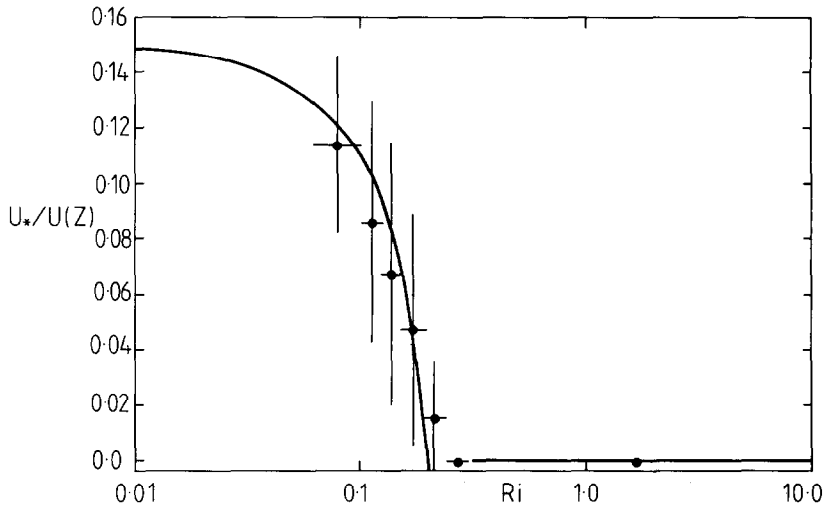

Fig. 1. The friction coefficient $u_*/u(z)$ at z = 13.7 m (level 4 at M2) as a function of gradient Richardson number Ri ($\bar{z}$ = 13.4 m at M1). Ri range is denoted by horizontal bar; vertical bar denotes standard deviation of individual data about mean. The continuous curve is based on Equation (4).

measured throughout the experiment at M2 at night showed the expected relation with Ri, *viz*, mean flux = 0 when Ri $\gtrsim$ 0.25. This is illustrated in Figure 1 for the case of u_* determined from eddy covariances, where we show the friction coefficient $u_*/u(z)$ as a function of Ri(z) with z = 13.7 m (level 4 at M2). Note that u_* and u are observed at M2 whilst Ri is inferred from profile data at M1. The continuous curve represents the inertial sub-layer relation

$$ku/u_* = \ln z/z_0 + \beta z/L \tag{4}$$

with $z/L \equiv \mathrm{Ri}/(1 - \beta\mathrm{Ri})$, β = 5, z_0 = 0.85 m and k, the von Karman constant, set equal to 0.41.

4. Surface-Layer Analysis

4.1 Observed gradients Φ_M^0

The observed non-dimensional gradients for wind are calculated from

$$\Phi_M^0 = (kz/u_*)\,\partial u/\partial z \tag{5}$$

using $u(z)$ at 5 levels on each of masts M1 and M2. We show in Figure 2 Φ_M^0 as a function of z/L for both M1 and M2, together with the inertial sub-layer relation (Equation (2)) with β = 5 and 7.5. The observations are also presented in Figure 3 in the form $\Phi_M^0/\Phi_M(z/L)$ as a function of z/h, where $\Phi_M(z/L)$ is given by Equation (2) with β = 5. This shows that the bulk of the observations are found with $z/L \lesssim 0.2$, and $z/h \lesssim 0.2$, with the upper levels probably lying above the surface layer on occasions. Two important features of the observations are evident in Figures 2, 3:

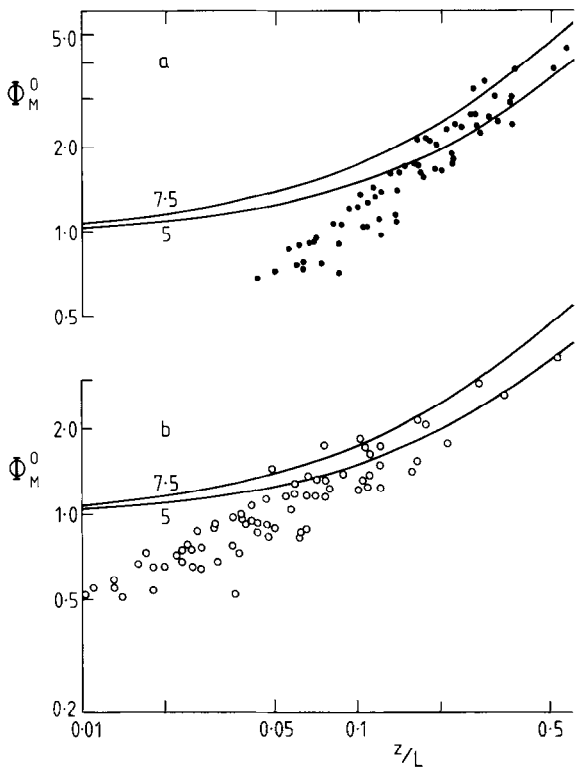

Fig. 2. Observed gradient Φ_M^0 as function of z/L: (a) at M1 (●) and (b) at M2 (○). Continuous curves represent $\Phi_M = 1 + \beta z/L$, with $\beta = 5$ and 7.5.

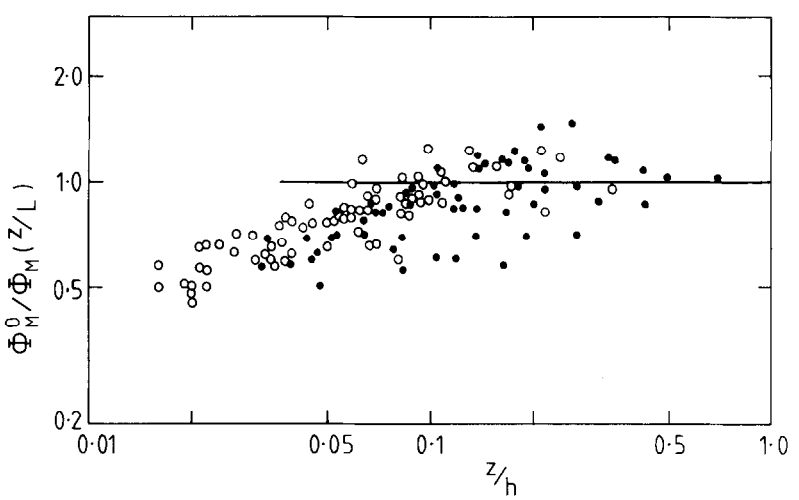

Fig. 3. Observed quantity $\Phi_M^0/\Phi_M(z/L)$ versus z/h, for M1 (●) and M2 (○) data, with $\Phi_M(z/L) = 1 + 5z/L$.

(i) Observed gradient Φ_M^0 is significantly less than inertial sub-layer values at small z/L ($\lesssim 0.1$);

(ii) Φ_M^0 tends to $\Phi_M(z/L)$ with $5 \lesssim \beta \lesssim 7.5$ at larger values of z/L.

These two aspects of the observations can be interpreted with the transition-layer concept, following the results of G80 for the daytime surface layer.

4.2. TRANSITION-LAYER DEPTH z_*

Garratt (1980) grouped the daytime data into small L ranges and, using Equation (1), applied 'least square' fits at each mast. These gave values of z_* and α_1 which were plotted as functions of L in Figures 4 and 5 of G80. There were no significant stability trends,

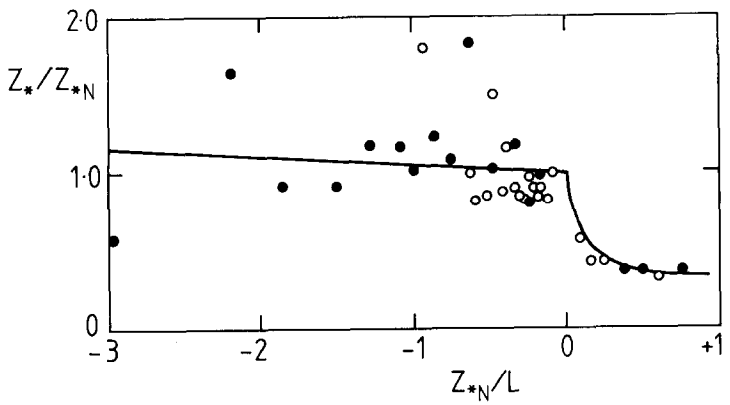

Fig. 4. Variation of observed normalised depth z_*/z_{*N} with stability z_{*N}/L, for M1 (●) and M2 (○). Continuous curve in unstable conditions is based on linear regression analysis.

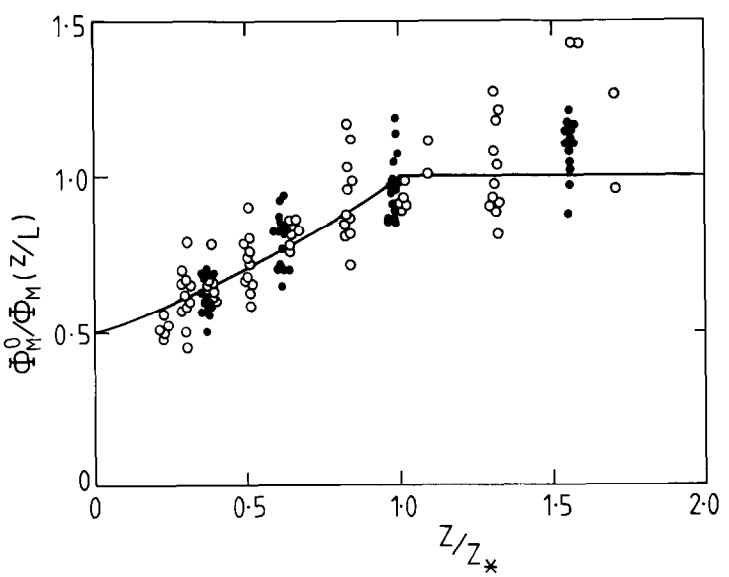

Fig. 5. Observed quantity $\Phi_M^0/\Phi_M(z/L)$ versus z/z_*, for M1 (●) and M2 (○) data, with $\Phi_M(z/L) = 1 + 5z/L$. Continuous curve for $z/z_* \leq 1$ represents Equation (6) with $\alpha_1 = 0.7$.

TABLE I

Estimated values of z_* at M1 and M2 for several L ranges, together with relevant NBL quantities.

Site	Mean L (m)	z_* (m)	z_*/z_{*_N}	z_{*_N}/L
M1	'neutral'	60	1.00	0.00
	160	22	0.37	0.38
	120	22	0.37	0.50
	80	22	0.37	0.75
M2	'neutral'	30	1.00	0.00
	350	17	0.57	0.09
	190	13	0.43	0.16
	125	13	0.43	0.24
	50	10	0.33	0.60

the implied neutral z_* values (denoted z_{*_N}) being 60 m at M1 and 30 m at M2, with $\alpha_1 \simeq 0.7$ at both sites.

Similar procedures have been followed with the present data sets using Equation (1) with $\Phi(z/L)$ defined by Equation (2) with $\beta = 5$. The parameter α_1 was again found to be $\simeq 0.7$, with no significant variations with L or between sites M1 and M2. Values of z_* are shown in Table I, together with several quantities relevant to the present discussion, and have an estimated uncertainty of approximately ± 5 m. Figure 4 shows the combined daytime and night-time data for M1 and M2, in the form z_*/z_{*_N} as a function of stability z_{*_N}/L (daytime data from G80). The curves are drawn to represent broadly the mean variation of z_* with stability.

At any one site, z_* in stable conditions is significantly smaller than the neutral value. This is physically plausible given that the surface-generated wakes which define the transition layer by their vertical penetration must do work against gravity. The decrease of z_* with increasing stability is analogous to the collapse of the ABL under the action of surface and clear-air radiative cooling.

4.3 Gradient function γ_M

Let γ_M represent $\Phi_M^0/\Phi_M(z/L)$ so that the proposed formula (cf. Equation (1)) is

$$\gamma_M = \exp\{-\alpha_1 (1 - z/z_*)\} \qquad z \leq z_* \tag{6}$$

with $\gamma_M = 1$ for $z \geq z_*$. These are shown in Figure 5 as continuous curves with $\alpha_1 = 0.7$, and compared with individual data, with $\Phi(z/L) = (1 + 5z/L)$, using values of z_* for each L range. The observed behaviour is similar to that of the daytime data shown in Figures (6–8) of G80.

However Equation (6) is different from the form assumed by Raupach *et al.* (1980) in describing neutral wind profiles (the analysis was done in terms of $u(z)$ rather than $\partial u/\partial z$) above rough surfaces in the wind tunnel. They assumed constant eddy diffusivity

in the transition layer, $= ku_*z_*$, implying $\gamma_M = z/z_*$, and giving

$$\frac{k}{u_*}(u(z) - u(z_*)) = -(1 - z/z_*) \qquad z < z_* \tag{7a}$$

compared with that derived from Equation (6), again for neutral conditions – e.g., Appendix 1 in G80 –

$$\frac{k}{u_*}(u(z) - u(z_*)) = \alpha \ln (z/z_*) \qquad z < z_* \tag{7b}$$
$$- \alpha\alpha_1(1 - z/z_*) - \ldots$$

where $\alpha_1 = 0.7$, $\alpha = \exp(-\alpha_1) = 0.5$.

Continuous curves representing Equation (7a) and (7b) are shown in Figure 6, which should be compared with Figure 11 of Raupach *et al.* (1980). The straight line represents the logarithmic law, with $k = 0.4$. Evidently the wake diffusion effect in the wind tunnel is somewhat greater than that over the Koorin surface although differences may in part be due to uncertainty in d, the zero-plane displacement. Pecked curves shown in the figure suggest that Equation (6) with $\alpha_1 = 1.05$ ($\alpha = 0.35$) most closely represents the wind-tunnel data.

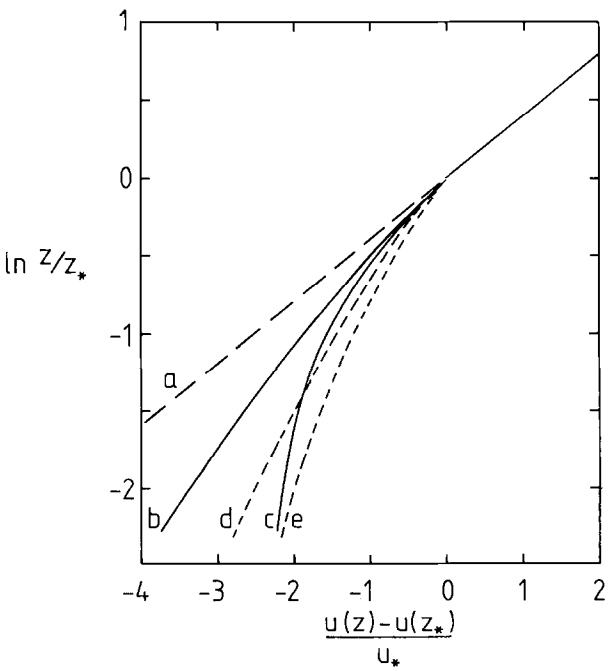

Fig. 6. Velocity profiles above a rough surface, with the curves described as follows: (a) logarithmic law, $k = 0.40$; (b) Equation (7b) with $\alpha = 0.5$, representing Koorin data; (c) Equation (7a) from Raupach *et al.* (1980) representing wind-tunnel data; (d) Equation (7b) with $\alpha = 0.35$ (hypothetical); (e) Equation (7b) with $\alpha = 0.25$ (hypothetical).

4.4 Dependence of analysis upon d

The sensitivity of Φ_M^0 to the assumed values of d has been discussed extensively by Hicks *et al.* (1979), Raupach (1979), Raupach *et al.* (1979), Garratt (1979, 1980). In the analyses of both unstable and stable data, we have taken most probable values of d (see G80), with no dependence upon stability. If such a dependence was admitted, less variation of z_* with stability would result for smaller values of d in unstable, and larger values in stable, conditions. Extreme values of d are limited by the ground ($d = 0$) and by the treetops ($d = 8$ m (M1) and 9.5 m (M2)). Influences on the stable-data analysis due to varying d are probably similar to those found by Garratt (1979) for the unstable analysis. Certainly a choice of $d \simeq 0$ removes systematic deviation of Φ_M^0 from $\Phi_M(z/L)$, but such a choice does not seem to be physically acceptable. At the other extreme, taking d at the treetops reduces Φ_M^0 still further below $\Phi_M(z/L)$, implying larger values of z_* (but still less than z_{*N}).

5. Conclusions

The transition-layer depth z_*, on the order of several tens of metres over the Koorin surface, is found to decrease significantly as stability increases. This is consistent with the well-known influences of stability upon inertial sub-layer and boundary-layer depths.

Inferences of the depth h_s from observed NBL depths suggest that the transition layer over our very rough surface occupies most of the inertial sub-layer when stably stratified.

Finally the gradient function

$$\gamma_M = \exp\{-\alpha_1 (1 - z/z_*)\}$$

with $\alpha_1 = 0.7$, and used by G80 to describe the unstable data, also describes the stable data.

Appendix: Calculation of Fluxes at M1

To calculate u_*, use has been made of the drag relation

$$u_* = \sqrt{C_D}\, u(\bar{z}) \tag{A1}$$

applied to the M1 layer between levels 4 and 5 ($\bar{z} = 34.3$ m). Here $u(\bar{z})$ is the observed layer mean wind speed and C_D can be expressed as the multiple of two terms: C_{DN}, the neutral drag coefficient ($= 0.0081$ for $z_0 = 0.4$ m) and a stability function readily calculated from the observed gradient Richardson number Ri (this assumes $z = 34.3$ m lies above the transition layer, an assumption confirmed by later analysis). In the case of H, an average of two estimates was taken for each run, the estimates being based on the following considerations. Firstly, the observed Ri implies a value of z/L and hence, with the calculated u_*, an estimate H_1. The second estimate used the analogous relation for heat flux to Equation (A1), viz.,

$$H_2 = \rho c C_H\, u(z)\,(\theta_0 - \theta(z)), \tag{A2}$$

where the neutral coefficient $C_{HN} = 0.0052$ for M1; ρ is air density and c the specific heat of air at constant pressure; $\theta(z)$ and θ_0 are the observed temperatures at z and the surface (radiometric), respectively. The assumed value of H is then given by $0.5\ (H_1 + H_2) \equiv \hat{H}$.

It is of interest to compare M1 estimates of u_* and H with those measured directly at M2. Firstly, consider the geostrophic wind relation (e.g., Arya, 1977)

$$u_*/G = \{(\ln h/z_0 - A)^2 + B^2\}^{-1/2}, \tag{A3}$$

where G is geostrophic wind, and A, B are known functions of the stability parameter h/L. Assuming both the observed h and G apply equally to M1 and M2, application of (A3) to both sites ($z_0 = 0.85$ m at M2), and taking $A = 1$, $B = 3$ for $h/L = 1.5$, gives

$$\overline{u}_*(\mathrm{M2})/\overline{u}^*(\mathrm{M1}) = 1.13$$

which compares favourably with the observed value of 1.1. Individual values are shown in Figure 7(a), with the straight line representing the above calculated ratio.

Secondly we compare M1 estimates of H (*viz.* $\hat{H}$) with those implied by surface energy balance at M1(H3) and with M2 values. The energy balance relation

$$H_3 = R - G - \lambda E \tag{A4}$$

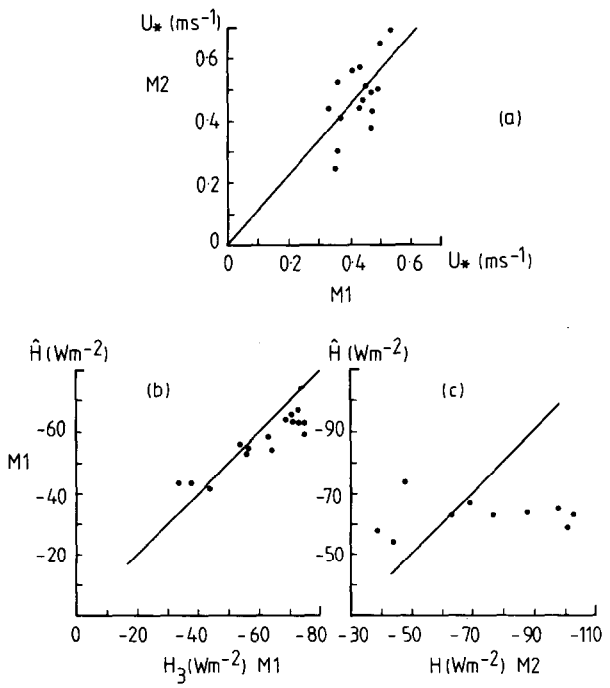

Fig. 7. Comparison of night-time u_* and H values: (a) u_* calculated at M1 vs. u_* observed at M2; the straight line represents the relation u_* (M2) = 1.13 u_* (M1) described in the text. (b) H calculated at M1 ($\hat{H}$) vs. value calculated from energy balance at M1 (H_3); a straight line of 45° slope is also shown. (c) $\hat{H}$ at M1 vs. observed value at M2 (this excludes Day 29 data); a straight line of 45° slope is also shown.

can be combined with the transfer relation for evaporation E, *viz*,

$$E = \frac{\rho(q_0^* - q(z))}{r_s + (C_H u(z))^{-1}}, \tag{A5}$$

where R is net radiation, G the surface soil heat flux, λ the latent heat of vaporisation, q_0^* is the saturated specific humidity at surface temperature and r_s is a 'surface' resistance given by Garratt (1978). Mean values at M1 of $\hat{H}$ and H_3 are -58 and -62 W m^{-2}, respectively, individual values plotted in Figure 7(b) showing good correlation. In addition, mean night-time values are comparable at M1 and M2 (-63 and -73 W m^{-2}, respectively), consistent with the near-equality in mean daytime values of 225 and 234 W m^{-2}. Individual values shown in Figure 7(c) do show however considerable differences, but this may be due, in part, to the space separation of the two masts.

Finally the data analysis excludes times immediately after the evening transition from unstable to stable boundary layer (18:00 and 19:00 local time), and at 23:00 on Day 7 and Day 27 when the sea-breeze perturbation is first apparent in the data as a whole. The measured and calculated fluxes used in the analysis are shown below.

Day	Time	Observed fluxes at M2		Calculated fluxes at M1	
		u_*	H	u_*	H
7	20:00	0.25	−44	0.35	−54
	21:00	0.43	−69	0.47	−67
	22:00	0.51	−63	0.45	−63
27	20:00	0.30	−39	0.36	−58
	21:00	0.38	−48	0.47	−74
	22:00	0.57	−77	0.43	−63
28	20:00	0.49	−101	0.47	−59
	21:00	0.50	−103	0.49	−63
	22:00	0.69	−98	0.53	−65
	23:00	0.65	−88	0.50	−64
29	00:00	0.56	(−61)	0.41	−53
	01:00	0.44	(−65)	0.43	−56
	02:00	0.46	(−63)	0.44	−54
	03:00	0.52	(−48)	0.36	−41
	04:00	0.41	(−50)	0.37	−43
	05:00	0.44	(−50)	0.33	−43

In the above, units of H and u_* are W m^{-2} and m s^{-1}, respectively; H values at M2 on Day 29 are based on M1 values, taking into account the difference in mean values found in the other data (Garratt, 1982).

References

Arya, S. P. S.: 1977, 'Suggested Revisions to Certain Boundary Layer Parameterization Schemes Used in Atmospheric Circulation Models', *Monthly Weather Rev.* **105**, 215–227.

Brost, R. A. and Wyngaard, J. C.: 1978, 'A Model Study of the Stably Stratified Planetary Boundary Layer', *J. Atmos. Sci.* **35**, 1427–1440.

Businger, J. A., Wyngaard, J. C., Izumi, Y., and Bradley, E. F.: 1971, 'Flux Profile Relationships in the Atmospheric Surface Layer', *J. Atmos. Sci.* **28**, 181–189.

Clarke, R. H. and Brook, R.R.: 1979, *The Koorin Expedition – Atmospheric Boundary Layer Data Over Tropical Savannah Land*, Department of Science, Canberra.

Garratt, J. R.: 1978, 'Transfer Characteristics for a Heterogeneous Surface of Large Aerodynamic Roughness', *Quart. J. Roy. Meteorol. Soc.* **104**, 491–502.

Garratt, J. R.: 1979, 'Comments on 'Analysis of Flux-Profile Relationships above Tall Vegetation – An Alternative View': II', *Quart. J. Roy. Meteorol. Soc.* **105**, 1079–1082.

Garratt, J. R.: 1980, 'Surface Influence Upon Vertical Profiles in the Atmospheric Near-Surface Layer', *Quart. J. Roy. Meteorol. Soc.* **106**, 803–819.

Garratt, J. R.: 1982, 'Observations in the Nocturnal Boundary Layer', *Boundary-Layer Meteorol.*, **22**, 21–48.

Garratt, J. R. and Brost, R. A.: 1981, 'Radiative Cooling Effects Within and above the Nocturnal Boundary Layer', *J. Atmos. Sci.* **38**, 2730–2746.

Hicks, B. B.: 1976, 'Wind Profile Relationships from the "Wangara" Experiment', *Quart J. Roy. Meteorol. Soc.* **102**, 535–551.

Hicks, B. B., Hess, G. D., and Wesely, M. L.: 1979, 'Analysis of Flux-profile Relationships above tall Vegetation ... an Alternative View', *Quart. J. Roy. Meteorol. Soc.* **105**, 1074–1077.

Monin, A. S. and Obukhov, A. M.: 1954, 'Basic Relationships of Turbulent Mixing in the Surface Layer of the Atmosphere'. *Acad. Nauk. SSr. Trud. Geofiz. Inst.* **24(151)**, 163–187.

Nieuwstadt, F. T. M. and Tennekes, H.: 1981, 'A Rate Equation for the Nocturnal Boundary Layer Height', *J. Atmos. Sci.* **38**, 1418–1428.

Raupach, M. R.: 1979, 'Anomalies in Flux-Gradient Relationships over Forest', *Boundary-Layer Meteorol.* **16**, 467–486.

Raupach, M. R., Stewart, J. B., and Thom, A. S.: 1979, 'Comments on "Analysis of Flux-Profile Relationships above tall Vegetation: An Alternative View": I'. *Quart. J. Roy. Meteorol. Soc.* **105**, 1077–1078.

Raupach, M. R., Thom, A. S., and Edwards, I.: 1980, 'A Wind-Tunnel Study of Turbulent Flow Close to Regularly Arrayed Rough Surfaces', *Boundary-Layer Meteorol.* **18**, 373–398.

Tennekes, H. and Lumley, J. L.: 1972, *A First Course in Turbulence*. M.I.T. Press, Cambridge, Mass.

Webb, E. K.: 1970, 'Profile Relationships: The Log-Linear Range and Extension to Strong Stability', *Quart. J. Roy. Meteorol. Soc.* **96**, 67–90.

Zeman, O.: 1979, 'Parameterization of the Dynamics of Stable Boundary Layers and Nocturnal Jets', *J. Atmos. Sci.* **36**, 792–804.